Structural and Electrical Characterization of SiO Gate Dielectrics Deposited From Solutions at Moderate Temperatures in Air

Mazran Esro, Oleg V. Kolosov, Peter John Jones, William I. Milne, and George Adamopoulos

Just Accepted

Structural and Electrical Characterization of SiO$_2$ Gate Dielectrics Deposited From Solutions at Moderate Temperatures in Air

Mazran Esro,[†+] *Oleg Kolosov,*[§] *Peter J. Jones,* [†] *William I. Milne,*[±×] *and George Adamopoulos*[†]*

[†] Engineering Department, Lancaster University, Lancaster LA1 4YR, UNITED KINGDOM

[+] Faculty of Electronics and Computer Engineering, Universiti Teknikal Malaysia Melaka (UTeM) Durian Tunggal, Melaka, 76100 MALAYSIA

[§] Department of Physics, Lancaster University, LA1 4YW, UNITED KINGDOM

[±] Department of Engineering, University of Cambridge, 9 JJ Thomson Avenue, Cambridge CB3 0FA, UNITED KINGDOM

[×] Quantum Nanoelectronics Research Center (QNERC), Tokyo Institute of Technology, 2-12-1 Ookayama, Meguro-ku, Tokyo, 152-8550, JAPAN

ABSTRACT: Silicon dioxide (SiO$_2$) is the most widely used dielectric for electronic applications. It is usually produced by thermal oxidation of silicon or by using a wide range of vacuum-based techniques. By default, the growth of SiO$_2$ by thermal oxidation of silicon, requires the use of Si substrates whereas the other deposition techniques either produce low quality or poor interface material and mostly require high deposition or annealing temperatures. Recent investigations

therefore have focused on the development of alternative deposition paradigms based on solutions. Here, we report the deposition of SiO_2 thin film dielectrics deposited by spray pyrolysis in air at moderate temperatures of ≈ 350 ^{o}C from pentane-2,4-dione solutions of $SiCl_4$. SiO_2 dielectrics were investigated by means of UV–Vis absorption spectroscopy, spectroscopic ellipsometry, XPS, XRD, UFM/AFM, admittance spectroscopy, and field-effect measurements. Data analysis reveals smooth ($R_{RMS} < 1$ nm) amorphous films with a dielectric constant of about 3.8, an optical band gap of ≈ 8.1 eV, leakage current densities in the order of $\approx 10^{-7}$ A/cm^2 at 1 MV/cm and high dielectric strength in excess of 5 MV/cm. XPS measurements confirm the SiO_2 stoichiometry and FTIR spectra reveal features related to SiO_2 only. Thin film transistors implementing spray coated SiO_2 gate dielectrics and C_{60} and pentacene semiconducting channels exhibit excellent transport characteristics i.e. negligible hysteresis, low leakage currents, high on/off current modulation ratio in the order of 10^6 and high carrier mobility.

1. INTRODUCTION

Despite the numerous dielectrics that have recently been developed, silicon dioxide (SiO_2) still remains the most common dielectric material used in the microelectronics field. The outstanding properties of SiO_2,[1,2] including excellent dielectric strength ($\approx 10^7$ V/cm), high resistivity ($\approx 10^{15}$ Ohms), large band gap (≈ 9 eV) plus its low interface defect density with Si, makes it critical for the current production of metal–oxide–semiconductor field effect transistors (MOSFETs). [3]

High quality SiO_2 films have traditionally been produced by thermal oxidation of Si at temperatures in the range between 900 ^{o}C and 1200 ^{o}C in O_2 or H_2O atmospheres. SiO_2 deposition at temperatures as low as room temperature on substrates other than silicon, has been the focus of research for many years.[4] Several alternative methods for SiO_2 deposition have been developed to

avoid the high deposition temperatures and long processing times. These deposition methods include wet chemical oxidation, chemical vapor deposition (CVD), magnetron sputtering, atomic layer deposition (ALD) and electron beam evaporation. Various publications have reported the production of SiO_2 using CVD, using a number of precursor materials systems and deposition temperatures. Excellent quality SiO_2 has been deposited by reaction of dichlorosilane and nitrous oxide[5] at ~900 ºC, silane and oxygen[6] at 200 ºC – 400 ºC or the decomposition of tetraethyl orthosilicate (TEOS) at 650 ºC – 800 ºC.[7-10] Plasma Enhanced Chemical Vapor Deposition (PECVD) in particular has often been used to lower film deposition temperatures.[4,11,12] However, the drawbacks to plasma processing include particle contamination as well as surface damage from the energetic plasma species. Additionally, novel and potentially expensive molecular precursors have also been explored for low temperature SiO_2 growth.[13] Catalyzed CVD of SiO_2 has also been used and much lower deposition temperatures have been achieved.[14,15] Atomic layer deposition (ALD), an alternative to CVD, has also gained considerable traction for the successful deposition of high quality SiO_2 films over a wide range of temperatures and substrates[16-18] and more recently, successful deposition of SiO_2 films from soluble precursors and further plasma treatment has also been reported.[19,20]

However, vacuum-based deposition techniques suffer from potential incompatibility with large area deposition and high manufacturing cost. Thus significant research has been focused on the development of alternative deposition methods from solutions. Indeed, solution processing techniques have produced a breakthrough in both cost and performance combined with high-throughput manufacturing. This has already been employed for the production of high quality dielectrics (mainly high-*k*) for implementation in TFTs using a number of solution produced active channel layers.[21-24]

In this report we demonstrate the deposition of SiO_2 gate dielectrics using spray coating, a simple and large area compatible technique at substrates temperature of about 350 °C. SiO_2 dielectrics were deposited onto commercially available ITO-coated glass, fused silica, KBr and c-Si substrates. The film properties were investigated using a number of characterization techniques including UV-Vis absorption spectroscopy, spectroscopic ellipsometry, X-ray diffraction, FTIR, x-ray photoelectron spectroscopy (XPS), impedance spectroscopy and AFM/UFM. TFT characteristics were obtained from bottom-gate, top-contact transistor architectures employing a spray coated SiO_2 gate dielectric and vacuum deposited C_{60} and pentacene semiconducting channels for organic n-MOS and p-MOS devices respectively.

2. EXPERIMENTAL SECTION

2.1. SiO_2 Deposition by Spray Pyrolysis: A 30 mg/ml precursor solution of silicon tetrachloride ($SiCl_4$) was prepared in pentane-2,4-dione and the solution was stirred at room temperature for 3 hours. The substrates were kept at 350 °C on a hotplate, while aerosols of the solution were sprayed sporadically onto the glass substrates employing a pneumatic airbrush, held at a distance of about 30 cm above the substrate. After a period of 20 s, the spraying process was interrupted for 30 s before the cycle was repeated until films of typical thicknesses in the range between 50 and 150 nm were obtained. This setup for the present combination of precursor material and solvent yielded films of excellent uniformity (thickness standard deviation < 2%) over an area of 15 cm x 15 cm. It was also found that at a substrate temperature of ≈350 °C films of excellent dielectric and optical properties were produced. Further increasing the deposition temperature (up to 500 °C) showed no effect on the optical and dielectric properties of the SiO_2 dielectric layer.

2.2. Organic semiconductors deposition: Sublimed-grade pentacene (purity > 99.9 %) and high purity fullerene (C_{60}) (>99.9 %) C_{60} films were deposited in a high-vacuum (10^{-7} mbar) Kurt J.

Lesker thermal evaporator onto spray coated glass/ITO/SiO_2 stacks at typical deposition rates of 0.1 nm s^{-1}. The thickness of each layer was measured by an *in-situ* quartz crystal monitor and further confirmed by spectroscopic ellipsometry.

2.3. Atomic force microscopy (AFM), ultrasonic force microscopy (UFM): Contact mode AFM was used to study the topography of the ITO and spray coated SiO_2 as well as thermally grown SiO_2. The measurements were performed in ambient conditions using a Bruker Nanoscope III, system and standard contact mode cantilevers (Contact-G, Budget Sensors, k = 0.2 N m^{-1}). UFM measurements were also carried out in ambience using a modified version of the above system and performed at a 4 MHz carrier frequency and 2.7 kHz modulation frequency using samples mounting on a 4 MHz thickness resonance piezoplate (PI) calibrated via a laser Doppler vibrometer (Polytec OFV-534).

2.4. X-ray Photoelectron Spectroscopy (XPS): XPS measurements of SiO_2 on ITO were conducted using a Thermofisher ESCALAB 250 electron spectrometer equipped with a hemispherical sector energy analyzer. An Al K_α x-ray source was used for analysis at source excitation energy of 15 keV and emission current of 6 mA. An analyzer pass energy of 20 eV with step size of 0.1 eV and dwell time of 50 ms was used throughout the experiments. The base pressure within the spectrometer during measurements was always lower than 5 x 10^{-10} mbar and this ensured that all signals recorded were from the sample surface with no contamination introduced from the vacuum chamber.

2.5. X-ray Diffraction: Grazing Incidence XRD (GIXRD) experiments were performed using a Rigaku SmartLab diffractometer with CuK_α radiation operating at 40 kV and 40mA.

2.6. UV–Vis Absorption Spectroscopy: Optical transmission spectra of SiO_2 on fused silica were measured at wavelengths between 200 nm and 1000 nm using an Agilent Cary 5000 spectrometer.

2.7. FTIR: The FTIR measurements of spray coated SiO_2 films on potassium bromide (KBr) substrates were conducted in transmission mode using a Perkin Elmer system 2000 Fourier transform spectrophotometer over a spectral range from 4000-400 cm^{-1} at a spectral resolution of 1 cm^{-1}.

2.8. Spectroscopic ellipsometry: SE measurements of SiO_2 films on intrinsic c-Si were performed in ambient conditions at an incidence angle of 70° using a Jobin–Yvon UVISEL phase modulated system over the spectral range 1 eV to 4.5 eV. The data were analyzed in terms of the Forouhi-Bloomer[25,26] model as modified by Jellison and Modine.[27] For the parameterization of the optical functions of SiO_2 the imaginary part of the dielectric function ε_2 is determined by multiplying the Tauc joint density of states by the ε_2 obtained from the Lorentz oscillator model:

$$\epsilon_2(E) = \begin{cases} \left[\dfrac{AE_0C(E-E_g)^2}{(E^2-E_0^2)^2+C^2E^2} \dfrac{1}{E} \right], E > E_g \\ \qquad\qquad\qquad 0, E < E_g \end{cases}$$

The four fitting parameters are E_g, A, E_0, and C and are in units of energy. The real part of the dielectric function ε_1 is obtained by Kramers–Kronig integration and an additional fitting parameter $\varepsilon_1(\infty)$ has been included.[27]

2.9. Impedance spectroscopy: Impedance spectroscopy measurements on Metal Insulator Metal (MIM) devices (glass/ITO/SiO_2/Au) were performed using a Solartron 1260 impedance/gain-phase analyzer at frequencies between 100 Hz and 10 MHz applying a 50 mV AC voltage. The Au electrodes were thermally evaporated on SiO_2 under high vacuum (10^{-7} mbar) through a shadow mask.

2.10. TFTs Fabrication/Characterization: Bottom Gate – Top Contact (BG–TC) transistors were then fabricated. Calcium and aluminum (Ca/Al) as well as gold (Au) source and drain (S/D) electrodes (50 nm) for n-MOS and p-MOS respectively were thermally evaporated under high

vacuum (10^{-7} mbar) through a shadow mask on the glass/ITO/SiO$_2$/organic layer stacks. The

devices employing C$_{60}$ and pentacene semiconducting channels were thermally annealed at 80 °C

in vacuum prior to characterization. Device characterization was carried out under high vacuum

(10^{-6} mbar), at room temperature using an Agilent B1500A semiconductor parameter analyzer.

Electron mobility was extracted from the transfer curves in both the linear and saturation regimes

using the gradual channel approximation:

$$\mu_{lin} = \frac{L}{C_i W V_D} \frac{\partial I_{DS}}{\partial V_{GS}}$$

$$\mu_{sat} = \frac{L}{C_i W} \frac{\partial^2 I_{DS}}{\partial^2 V_{GS}}$$

3. RESULTS AND DISCUSSION

The UV-Vis transmission spectra of SiO$_2$ films spray coated on fused silica substrates at 350 °C

are shown in Figure 1a. The spectra demonstrate films of high optical quality with an average

transmittance (%) in the visible (400 nm – 700 nm) of about 97 %. As expected though, no optical

transitions of the SiO$_2$ films near the band edge were observed at such low photon energies. As a

result, the optical properties of SiO$_2$ films were further investigated by ex situ UV–Visible

spectroscopic ellipsometry in the range of photon energies from 1 to 4.5 eV.

As discussed, parameterization of the dielectric functions of SiO$_2$ (or amorphous materials in

general) in the near UV to near IR range is based on the quantum mechanical or Lorentz oscillator

and the Tauc joint density of states model initially developed by Forouhi and Bloomer[25,26]

McGahan and Woolam[27] and modified by Jellison and Modine to address certain issues and correct

some errors and inconsistencies.[28] It should be noted though that this parameterization includes

only interband transitions. Any Urbach tail absorption, intraband absorption or defect absorption, ,

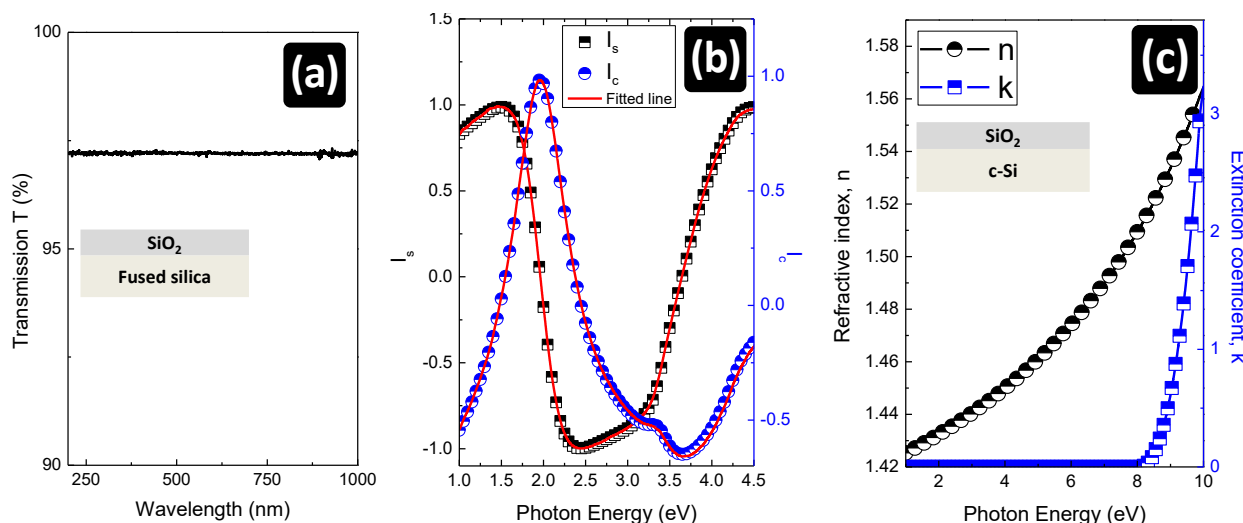or are not explicitly included in the model.

Figure 1: a) Transmittance T% in the photon range between 200 nm and 1000 nm of SiO_2 sprayed coated at ≈350 °C on fused silica substrates. **b)** Experimental data and fitted lines of the parameters I_S=sin2Ψsin∆ and I_C= sin2Ψcos∆ of SiO_2 films sprayed at ≈350 °C on silicon substrates. The fitted lines were calculated by means of a modified version of the Forouhi–Bloomer model[27] and the effective-medium approximation **c)** Refractive index and extinction coefficient of SiO_2 films spray coated at ≈350 °C as derived from spectroscopic ellipsometry.

For SiO_2 films, one oscillator (only five parameters are needed, see experimental section) provides

an excellent fit to the data as shown in Figure 1b. The "extended to high energies" refractive index

(n) and extinction coefficient (k) dispersions are illustrated in Figure 1c. The optical band gap (as

derived by extrapolation) was found to be ≈8.11 eV consistent with the values calculated for

thermally grown SiO_2 (≈8.13) measured under the same conditions. Additionally, the infinite

dielectric constant (ε_∞) was found to be ≈18.5 yielding in turn a pinning factor S[29] of 0.94,

comparable with the reported values for thermally grown SiO_2.[30]

X-ray diffraction revealed amorphous films (no features of crystalline SiO_2) and thus the

microstructure of the spray coated SiO_2 films on KBr was further investigated by FTIR. The IR

spectra of both the precursor solution ($SiCl_4$ in pentane-2,4-dione) as well as the SiO_2 film that was deposited at 350 ^{o}C are shown in Figure 2a. One can immediately observe the lack of any features due to impurities or residual species (pentane-2,4-dione or $SiCl_4$) in the SiO_2 film spectrum. Only four prominent peaks are present i.e. the Si–O out-of-plane rocking mode at ≈460 cm^{-1}, the Si–O bending mode at ≈800 cm^{-1}, and the Si–O and Si–O–Si stretching modes at ≈1080 cm^{-1} and ≈1200 cm^{-1} respectively.[31] In addition, the FTIR spectrum of the SiO_2 films reveals no (or extremely weak) features at 3400 cm^{-1} or at 3650 cm^{-1} which would correspond to the H–O–H and the Si–O–H stretching modes respectively. This further confirms that no OH groups were incorporated into the SiO_2 film during or after deposition. Further analysis of the FTIR spectra in the range between 1450 cm^{-1} and 1850 cm^{-1} provides more details on the structure of the precursor solution. Indeed, Figure 2b provides evidence of the reaction between pentane-2,4-dione and $SiCl_4$ to yield tris-(2,4-pentanedione)-silicon chloride HCl, a compound with a decomposition temperature in the range between 170 ^{o}C and 174 ^{o}C[32]. Tris-(2,4-pentanedione)-silicon chloride 1-hydrogen chloride shows no infrared absorption in the carbonyl region near 1700 cm^{-1}, and instead has a single very strong and broad absorption band at about 1555 cm^{-1}. This intensity enhancement and very large shift of the C-O absorption band can only be accounted for by assuming that the carbonyl oxygens form strong complexes with an acidic site, which should in this case be the silicon atom. Such absorption behavior was found in metal chelates, all of which show strong bands in the 1500-1600 cm^{-1} region.[32] We equally conclude that our precursor solution is a compound whose structure has three acetylacetonate groups which are chelated about a silicon ion, occupying six $3s3p^33d^2$ hybrid orbitals octahedrally distributed about the silicon.
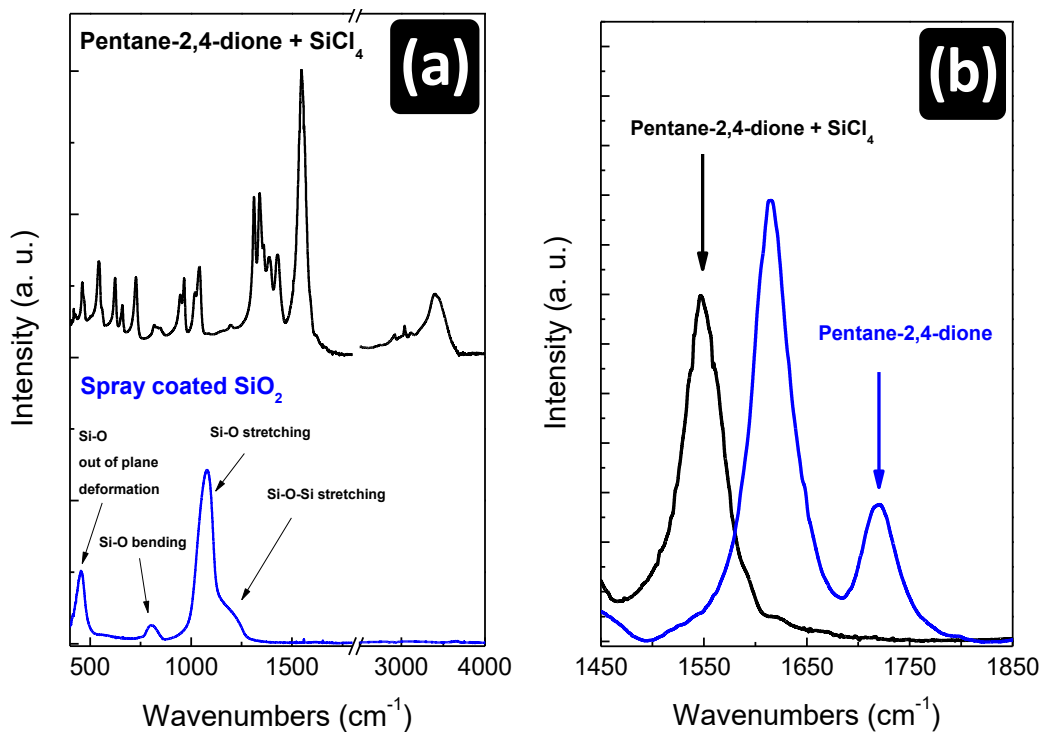
Figure 2: a) FTIR spectra in the region between 400 cm^{-1} and 4000 cm^{-1} of the precursor solution (SiCl$_4$ in pentane-2,4-dione) and SiO$_2$ films deposited by spray pyrolysis on KBr substrates. The spectra confirm complete decomposition of the precursors and further confirm SiO$_2$ deposition. The SiO$_2$ shows four prominent peaks i.e. the Si–O out-of-plane rocking mode at $\approx$460 cm^{-1}, the Si–O bending mode at $\approx$800 cm^{-1}, and the Si–O and Si–O–Si stretching modes at $\approx$1080 cm^{-1} and $\approx$1200 cm^{-1} respectively. **b)** FTIR spectra in the region between 1450 cm^{-1} and 1850 cm^{-1} of the precursor solution (SiCl$_4$ in pentane-2,4-dione) and the pentane-2,4-dione solvent. The absence of the infrared absorption band in the carbonyl region near 1700 cm^{-1}, and instead the single very strong and broad absorption band at about 1555 cm^{-1} indicate the formation of Tris-(2,4-pentanedione)-silicon chloride HCl in the precursor solution.

The films' stoichiometry was further investigated by X-ray photoelectron spectroscopy so that more information on the Si-O bonding energies and elemental composition could be obtained and confirmed that stoichiometric SiO$_2$ was indeed formed. The XPS spectrum of spray coated SiO$_2$ in the energy range between 10 eV and 1350 eV is illustrated in Figure 3a.
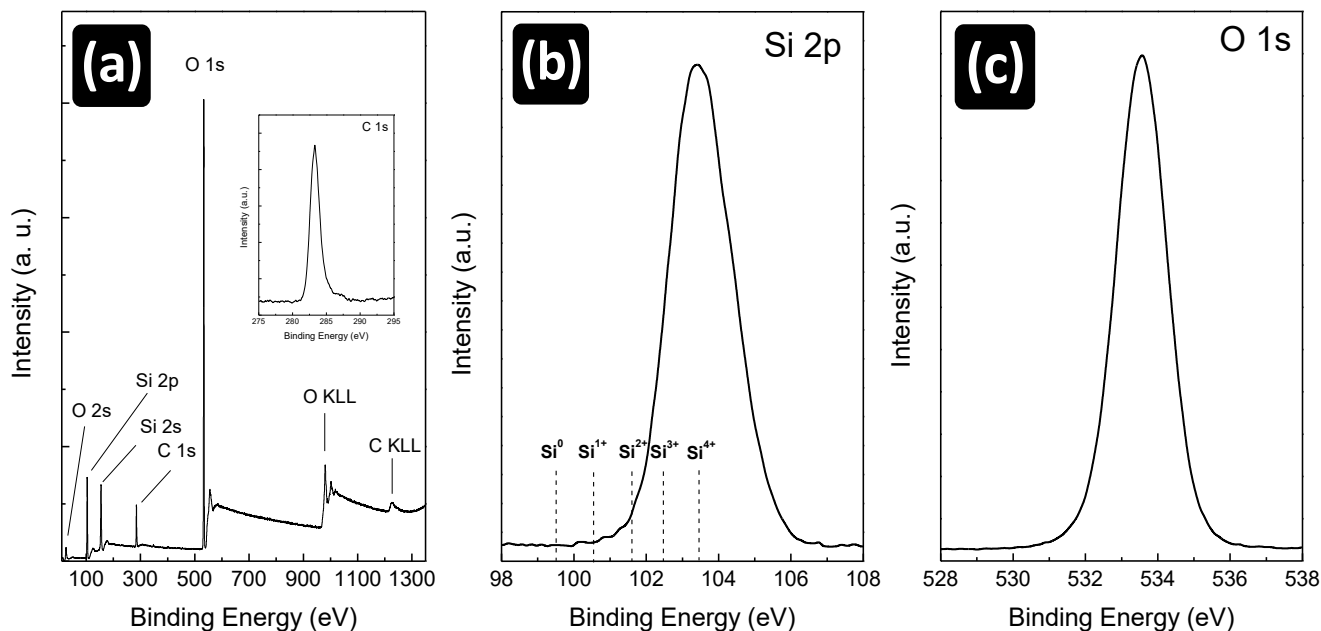
Figure 3: a) Wide scan XPS spectra of SiO_2 films (~130 nm) sprayed coated at ~350 ^{o}C on silicon substrates (**inset**: C 1s core level curve). High resolution **b)** Si 2p and **c)** O 1s XPS spectra.

The main peaks observed were the Si 2p, Si 2s, C 1s and O 1s photoemission peaks at binding energies of ~104, 150, 285 and 533 eV respectively, with O and C Auger *KLL* peaks at 990 eV and 1225 eV respectively. No features from any other elements contributed to the spectrum. Further narrow region energy scans allowed determination of the chemical state of the specific element identified as depicted in Figure 3b, and Figure 3c as Si 2p and O 1s respectively. Figure 3b clearly demonstrates that the dominant chemical structure is that of the Si^{4+} oxidation state that corresponds to SiO_2. Additionally, the absence of any features at 99.5 eV (Si^0)[33,34] further confirms the precursor's conversion to SiO_2. Last but not least, the relative atomic concentration ratio Si:O was calculated from the intensities of the major photoelectron spectral lines by means of codes incorporated in the instrument data system using Scofield cross sections[35] and found to be 0.5 further confirming SiO_2 growth.

The surface morphologies of an ITO coated glass substrate, spray coated SiO_2 on ITO coated glass and a 400 nm reference thermal oxide were investigated by atomic force microscopy (AFM) and ultrasonic force microscopy (UFM).[36,37] UFM uses the standard contact AFM setup combined with

a high frequency (MHz) but very small amplitude (sub-nm) ultrasonic vibration applied to the device. The oscillating strain field propagates to the subsurface of the sample equally probing the integrity of buried structures and interfaces and provides high sensitivity nanoscale resolution mapping of solid state materials with a wide range of elastic moduli (from 100 MPa to several 100s GPa). Moreover, the surface damage to the sample and the tip during UFM imaging is negligible because of the effect of ultrasound-induced lubricity that eliminates the shear forces during the scanning.[38]

AFM and UFM topography images of the ITO coated glass substrate, spray coated SiO_2 and thermally grown SiO_2 are depicted in Figure 4. The images presented are the raw images as further image processing (e.g. for tip dilation) was omitted as it showed no improvement of the image quality. The films' surface was investigated in terms of root-mean-square roughness and found to be $\approx$1.21 nm for ITO considerably higher than those of spray coated ($\approx$0.55 nm) SiO_2 (on ITO) and thermally grown ($\approx$0.15 nm) SiO_2. The obvious differences in films morphology indicate that the SiO_2 surface morphology and growth is dominated by the deposition process rather than the morphology of the underlying ITO-coated glass substrate. This low surface roughness for the spray coated SiO_2 (comparable to that of thermally grown SiO_2) constitutes a promising finding for the implementation of spray coated SiO_2 dielectrics into thin film transistors.
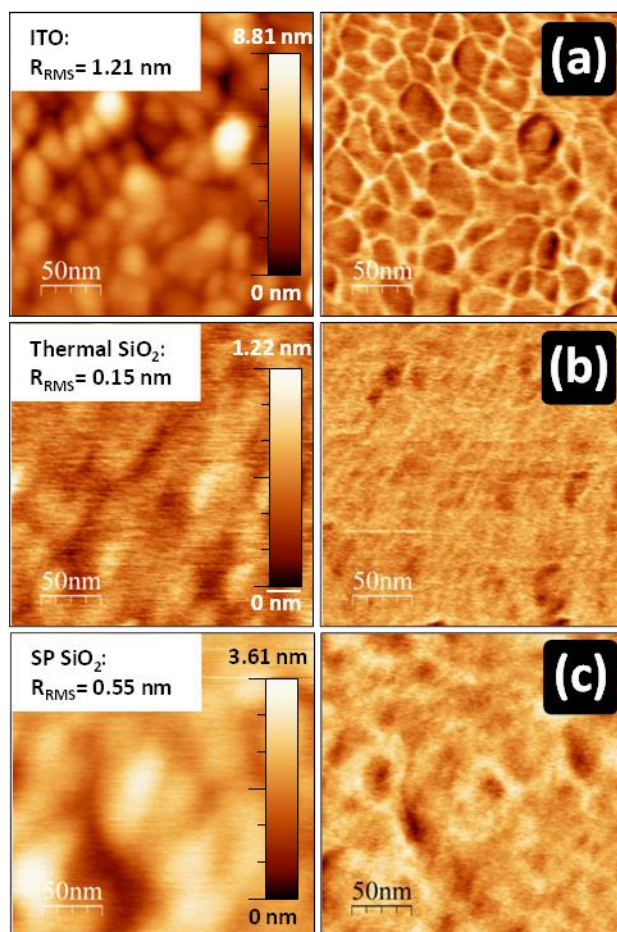
Figure 4: AFM and UFM topography images (and R_{RMS} roughness inset) of **a)** commercially available ITO, **b)** Thermally grown SiO_2, and **c)** SiO_2 films on ITO spray coated at $\approx 350\ ^oC$ in air.

The leakage currents and dielectric properties of SiO_2 films were obtained by employing a metal-insulator-metal device architecture. Spray coated SiO_2 films of thickness of ~130 nm were sandwiched between ITO and Au electrodes (inset Figure 5a). The static dielectric constant dispersion in the frequency range between 100 Hz and 10 MHz is shown in Figure 5a. The Nyquist plot as well as the dissipation factor (DF), are illustrated in the inset in Figure 5a and in Figure 5b respectively. The static dielectric constant as derived by the geometric capacitance at 100 Hz (extracted from the Bode plot) was found to be ≈ 3.8 in very good agreement with that reported (3.9) for SiO_2. The dissipation factor (DF) was found to be as small as 0.1 at low frequencies,

indicating excellent capacitive properties. The DF resonance at about 4 MHz is attributed to dipole

relaxation. In addition, the Nyquist plot (inset Figure 5a) reveals a stable system whose equivalent

circuit consists of a capacitor with high shunt and low series resistance.
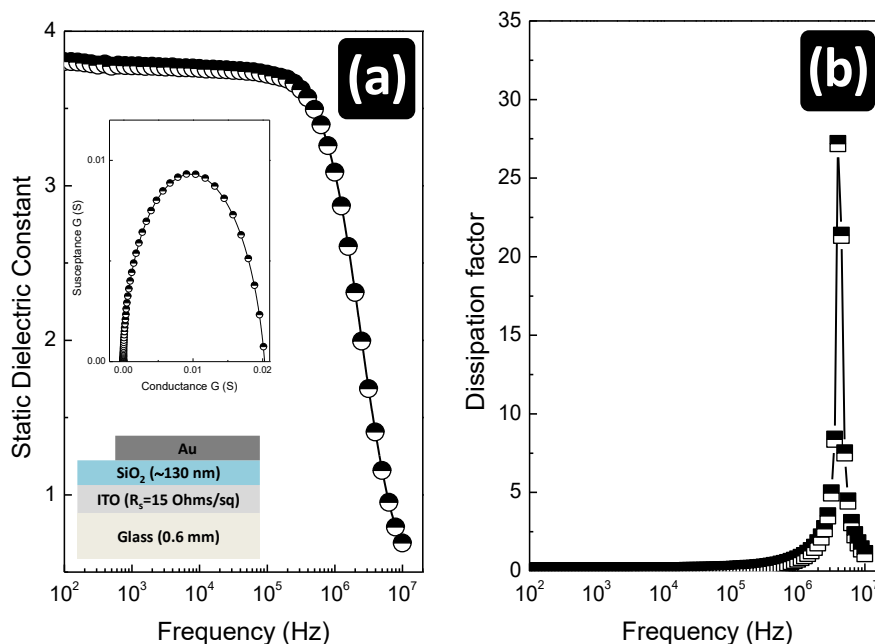
Figure 5: a) Dielectric constant dispersion in the frequency range between 100 Hz and 10 MHz (inset, Nyquist plot and MIM device architecture) and **b)** Dissipation factor of SiO_2 films at $\approx$350 $^{\circ}$C in air.

The current density versus electric field characteristics of the same MIM device (ITO/SiO_2

($\approx$130 nm)/Au($\approx$100 nm)) are shown in Figure 6a. As shown, the devices exhibit excellent

dielectric strength and no dielectric breakdown was observed for electric fields as high as 5

MV cm^{-1}. In an effort to determine the leakage current mechanism, Figures 6b and 6c show

the Fowler Nordheim (F-N) and Poole-Frenkel (P-F) plots of the same characteristics. Both F-

N and P-F plots shows some linearity at high electric field indicating that the conduction could

equally be determined by either F–N tunneling (i.e. an interface limited process) or P-F i.e.

bulk-limited. Based on the data illustrated in Figure 6, and given the linearity over a limited

electric field range for both plots, we can't safely decide upon the dominant conduction mechanism. Figure 2c, certainly infers the presence of trap states and barrier height lowering at high electric fields however the origin of such trap states, previously associated with nano-porous SiO_2 films deposited by sol-gel[39], remains unknown and such a hypothesis is not supported by UFM measurements (Figure 4c) that show porous-free films. A F-N dependence has been observed for thermally grown SiO_2,[40] and a Poole-Frenkel type (i.e. bulk limited) of conduction has also been reported for SiO_2 that was deposited from solutions and treated with plasma.[41] Further measurements on the temperature dependence of the plots would help to clarify the situation, however such detailed investigation is outside the scope of the present study.
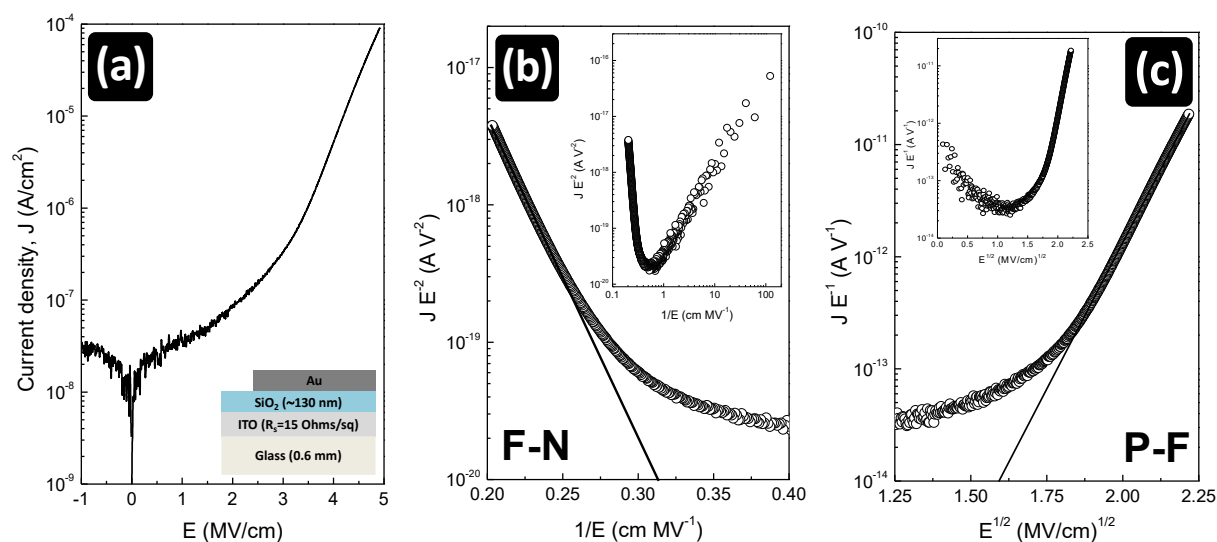

Figure 6: a) Leakage current density **b)** Fowler-Nordheim plot (inset: extended Fowler-Nordheim plot) and **c)** Poole-Frenkel plot (inset: extended Poole-Frenkel plot) of a ≈130 nm SiO_2 MIM device deposited by spray pyrolysis at ≈350 ℃.

Finally, Figure 7 depicts the band gap and static dielectric constant of a wide range of dielectric materials (including the findings of the present study) grown by a wide range of deposition

techniques, including solution processed ones, further demonstrating the well-established

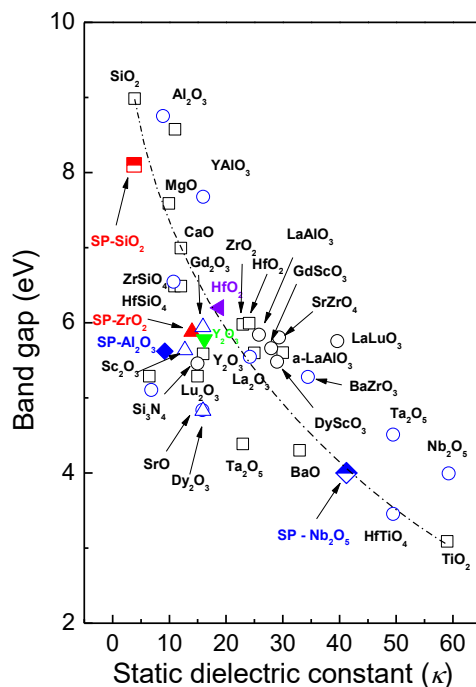dielectric constant-band gap trend of both vacuum[42,43] and solution processed gate dielectrics.[21]

Figure 7: Static dielectric constant vs band gap for oxide gate dielectric grown by a wide range deposition methods both vacuum and solutions based.

The performance of spray coated SiO_2 films as a gate dielectric was investigated in a bottom-gate, top-contact (BG–TC) TFT architecture (inset, Figure 8 and 9) employing C_{60} and pentacene as channel semiconductors. The organic layers as well as the source and drain contacts were evaporated under high vacuum conditions as described in the experimental section. The devices were measured under vacuum immediately after deposition.
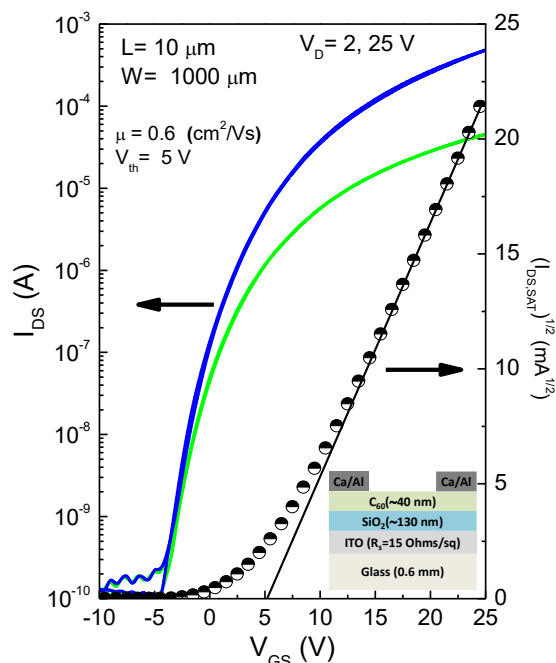
Figure 8: Linear (V_{DS} = 2 V) and saturated (V_{DS} = 25 V) transfer characteristics of bottom-gate, top-contact (inset: architecture employed) TFTs with channel width W= 1000 µm and channel length L = 10 µm, employing an evaporated C_{60} semiconducting channel on a $\approx$26 nF/cm^2 spray coated SiO_2 dielectric.

Figures 8 and 9 show a representative set of transfer characteristics obtained from C_{60} and pentacene TFTs (L = 10 μm, W = 1000 μm) based on a ~130 nm ($C_{ox} \approx$ 26 nF/cm^2) thick SiO_2 dielectric. The devices exhibit excellent operating characteristics with low voltage operation, negligible hysteresis, high on/off current modulation ratio in the order of 10^6 and high carrier mobility of approximately 0.6 cm^2 V^{-1} s^{-1} and 0.02 cm^2 V^{-1} s^{-1} for C_{60} and pentacene TFT respectively.
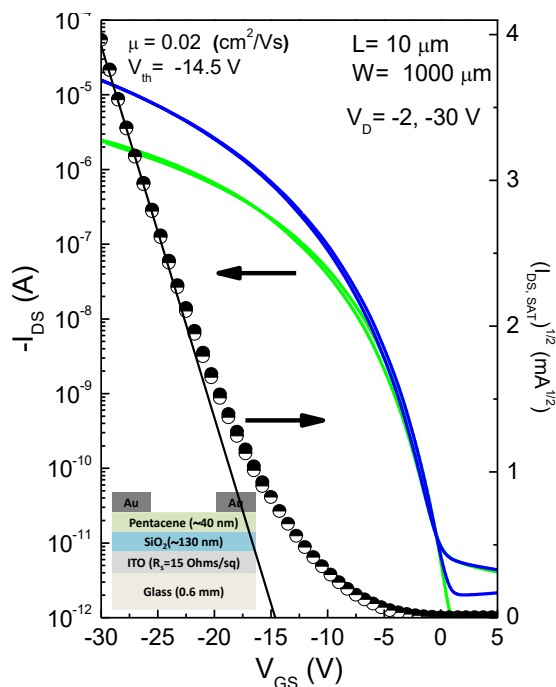
Figure 9: Linear (V_{DS} = -2 V) and saturated (V_{DS} = -30 V) transfer characteristics of bottom-gate, top-contact (inset: architecture employed) TFTs with channel width W= 1000 µm and channel length L = 10 µm, employing a pentacene semiconducting channel on a ≈26 nF/cm² spray coated SiO₂ dielectric.

4. CONCLUSION

We have demonstrated the production of solution processed SiO₂ dielectrics over large areas under ambient conditions at moderate substrate temperatures of ≈350 °C and their implementation in (both electron and hole transporting) TFTs employing organic semiconducting channels. The films were spray coated from silicon chloride blends in pentane-2,4-dione and the films' physical properties were investigated by a wide range of characterization techniques that demonstrated the production of ultra-smooth amorphous SiO₂ films, with wide band gap, dielectric constant similar to that of thermally grown SiO₂ and similar leakage currents. The TFTs that were manufactured using SiO₂ layers as gate dielectrics showed excellent characteristics in terms of carrier mobilities (both electrons and holes), negligible hysteresis, and high on/off current ratios.

Finally, the excellent reproducibility and films' homogeneity, combined with the relatively low - for SiO₂- deposition temperature in ambient air on substrates other than silicon, indicates the

1
2
3
4
5
6
7
8
9
10
11
12
13
14
15
16
17
18
19
20
21
22
23
24
25
26
27
28
29
30
31
32
33
34
35
36
37
38
39
40
41
42
43
44
45
46
47
48
49
50
51
52
53
54
55
56
57
58
59
60

potential for the rapid development of organic TFTs on SiO_2 gate dielectrics grown from solutions at low manufacturing cost.

AUTHOR INFORMATION

Corresponding Author

*Dr George Adamopoulos. Email: g.adamopoulos@lancaster.ac.uk

Notes

The authors declare no competing financial interest.

REFERENCES

(1)   Green, M. L.; Gusev, E. P.; Degraeve, R.; Garfunkel, E. L. Ultrathin (<4 Nm) SiO_2 and Si-O-N Gate Dielectric Layers for Silicon Microelectronics: Understanding the Processing, Structure, and Physical and Electrical Limits. *J. Appl. Phys.* **2001**, *90* (5), 2057–2121.

(2)   Helms, C. R.; Poindexter, E. H. *T*he Silicon-Silicon-Dioxide System : Its Microstructure and Imperfections. *Rep. Prog. Phys.* **1994**, *57*, 791–852.

(3)   Gusev, E. P.; Lu, H.-C.; Garfunkel, E. L.; Gustafsson, T.; Green, M. L. Growth and Characterization of Ultrathin Nitrided Silicon Oxide Films. *IBM J. Res. Dev.* **1999**, *43*, 265–286.

(4)   Klaus, J. W.; Sneh, O.; George, S. M. Growth of SiO_2 at Room Temperature with the Use of Catalyzed Sequential Half-Reactions. *Science* **1997**, *278*, 1934–1936.

(5)   Watanabe, K.; Tanigaki, T.; Wakayama, S. The Properties of LPCVD SiO_2 Film Deposited by SiH_2Cl_2 and N_2O Mixtures. *J. Electrochem. Soc.* **1981**, *128*, 2630–2635.

(6)   Kern, W.; Rosler, R. S. Advances in Deposition Processes for Passivation Films. *J. Vac.*

Sci. Technol. **1977**, *14*, 1082-1099.

(7)   Becker, F. S.; Pawlik, D.; Anzinger, H.; Spitzer, A. Low-pressure Deposition of High-quality SiO_2 Films by Pyrolysis of Tetraethylorthosilicate. *J. Vac. Sci. Technol. B* **1987**, *5,* 1555-1563.

(8)   Hamelmann, F.; Heinzmann, U.; Szekeres, A.; Kirov, N.; Nikolova, T. Deposition of Silicon Oxide Thin Films in TEOS with Addition of Oxygen to the Plasma Ambient: IR Spectra Analysis. *J. Optoelectron. Adv. Mater.* **2005**, *7*, 389–392.

(9)   Kim, J.; Hwang, S.; Yi, J. SiO_2 Films Deposited at Low Temperature by Using APCVD with $TEOS/O_3$ for TFT Applications. *J. Korean Phys. Soc.* **2006**, *49*, 1121–1125.

(10)   Rha, S.; Chou, T. P.; Cao, G.; Lee, Y.; Lee, W. Characteristics of Silicon Oxide Thin Films Prepared by Sol Electrophoretic Deposition Method Using Tetraethylorthosilicate as the Precursor. *Curr. Appl. Phys.* **2009**, *9*, 551–555.

(11)   Rashid, R.; Flewitt, A. J.; Grambole, D.; Kreiβig, U.; Robertson, J.; Milne, W. I. High Quality Growth of SiO_2 at 80° C by Electron Cyclotron Resonance (ECR) for Thin Film Transistors. *MRS Online Proc. Libr.* **2001**, *685*, D13.1.1.

(12)   Hamakawa, M. O. and Toyoda, Y. Photo-Induced Chemical Vapor Deposition of SiO_2 Film Using Direct Excitation Process by Deuterium Lamp. *Jpn. J. Appl. Phys.* **1984**, *23*, L97-L99.

(13)   Masakiyo Matsumura, S. M. and Y. U. and. Atomic-Layer Chemical-Vapor-Deposition of SiO_2 by Cyclic Exposures of $CH_3OSi(NCO)_3$ and H_2O_2. *Jpn. J. Appl. Phys.* **1995**, *34*, 5738-5742.

(14)   Tripp, C. P.; Hair, M. L. Chemical Attachment of Chlorosilanes to Silica: A Two-Step Amine-Promoted Reaction. *J. Phys. Chem.* **1993**, *97*, 5693–5698.

(15)   Blitz, J. P.; Murthy, R. S. S.; Leyden, D. E. Ammonia-Catalyzed Silylation Reactions of Cab-O-Sol with Methoxymethylsilanes. *J. Am. Chem. Soc.* **1987**, *109*, 7141–7145.

(16)   Dingemans, G.; Helvoirt, C. A. A. Van; Pierreux, D.; Keuning, W.; Kessels, W. M. M. Plasma-Assisted ALD for the Conformal Deposition of SiO_2 : Process , Material and Electronic Properties. *J. Electrochem. Soc.* **2012**, *159* (3), H277–H285.

(17)   Burton, B.; Boleslawski, M. Rapid SiO_2 Atomic Layer Deposition Using Tris (Tert-Pentoxy) Silanol. *Chem. Mater.* **2008**, *20*, 7031–7043.

(18)   Burton, B. B.; Kang, S. W.; Rhee, S. W.; George, S. M. SiO_2 Atomic Layer Deposition Using Tris (Dimethylamino) Silane and Hydrogen Peroxide Studied by in Situ Transmission FTIR Spectroscopy. *J. Phys. Chem. C.* **2009**, *113*, 8249–8257.

(19)   Jeong, Y.; Pearson, C.; Kim, H.; Park, M.; Kim, H.; Do, L.; Petty, M. C. Optimization of a Solution-Processed SiO_2 Gate Insulator by Plasma Treatment for Zinc Oxide Thin Film Transistors. *ACS Appl. Mater. Interfaces* **2016**, *8*, 2061–2070.

(20) Jeong, Y.; Pearson, C.; Kim, H.-G.; Park, M.-Y.; Kim, H.; Do, L.-M.; Petty, M. C. Solution-Processed SiO_2 Gate Insulator Formed at Low Temperature for Zinc Oxide Thin-Film Transistors. *RSC Adv.* **2015**, *5*, 36083–36087.

(21) Esro, M.; Vourlias, G.; Somerton, C.; Milne, W. I.; Adamopoulos, G. High-Mobility ZnO Thin Film Transistors Based on Solution-Processed Hafnium Oxide Gate Dielectrics. *Adv. Funct. Mater.* **2015**, *25*, 134–141.

(22) Adamopoulos, G.; Thomas, S.; Bradley, D. D. C.; McLachlan, M. A.; Anthopoulos, T. D. Low-Voltage ZnO Thin-Film Transistors Based on Y_2O_3 and Al_2O_3 High-K Dielectrics Deposited by Spray Pyrolysis in Air. *Appl. Phys. Lett.* **2011**, *98*, 123503-1 - 123503-3.

(23) Adamopoulos, G.; Thomas, S.; Wöbkenberg, P. H.; Bradley, D. D. C.; McLachlan, M. A.; Anthopoulos, T. D. High-Mobility Low-Voltage ZnO and Li-Doped ZnO Transistors Based on ZrO_2 High-K Dielectric Grown by Spray Pyrolysis in Ambient Air. *Adv. Mater.* **2011**, *23*, 1894–1898.

(24) Afouxenidis, D.; Mazzocco, R.; Vourlias, G.; Livesley, P. J.; Krier, A.; Milne, W. I.; Kolosov, O.; Adamopoulos, G. ZnO-Based Thin Film Transistors Employing Aluminum Titanate Gate Dielectrics Deposited by Spray Pyrolysis at Ambient Air. *ACS Appl. Mater. Interfaces* **2015**, *7*, 7334–7341.

(25) Forouhi, A. R.; Bloomer, I. Optical Dispersion Relations for Amorphous Semiconductors and Amorphous Dielectrics. *Phys. Rev. B* **1986**, *34*, 7018–7026.

(26) Forouhi, A. R.; Bloomer, I. Optical Properties of Crystalline Semiconductors and Dielectrics. *Phys. Rev. B* **1988**, *38*, 1865–1874.

(27) McGahan, W. A.; Makovicka, T.; Hale, J.; Woollam, J. A. Modified Forouhi and Bloomer Dispersion Model for the Optical Constants of Amorphous Hydrogenated Carbon Thin Films. *Thin Solid Films.* **1994**, *253*, 57–61.

(28) Jellison, G. E.; Modine, F. A. Parameterization of the Optical Functions of Amorphous Materials in the Interband Region. *Appl. Phys. Lett.* **1996**, *69*, 371-373.

(29) Mönch, W. Role of Virtual Gap States and Defects in Metal-Semiconductor Contacts. *Phys. Rev. Lett.* **1987**, *58*, 1260–1263.

(30) Robertson, J. Band Offsets of Wide-Band-Gap Oxides and Implications for Future Electronic Devices. *J. Vac. Sci. Technol. B* **2000**, *18* (3), 1785-1791.

(31) Zacharias, M.; Dlmova-malinovska, D.; Stutzmann, M. Properties of Hydrogenated Amorphous Silicon Suboxide Alloys with Visible Room-Temperature Photoluminescence. *Philos. Mag. Part B* **1996**, *73* (5), 799–816.

(32) West, R. Silicon and Organosilicon Derivatives of Acetylacetone. *J. Am. Chem. Soc.*, **1958**, 80 (13), pp 3246–3249.

(33) Kim, S.; Kim, M. C.; Choi, S.; Kim, K. J.; Hwang, H. N.; Hwang, C. C.; Kim, S.; Kim, M. C.; Choi, S. Size Dependence of Si 2P Core-Level Shift at Si Nanocrystal/SiO_2 Interfaces.

Appl. Phys. Lett. **2007**, 91, *103113-1 - 103113-3*.

(34) Kim, K. J.; Kim, J. W.; Yang, M. S.; Shin, J. H. Oxidation of Si during the Growth of SiOx by Ion-Beam Sputter Deposition: In Situ X-Ray Photoelectron Spectroscopy as a Function of Oxygen Partial Pressure and Deposition Temperature. *Phys. Rev. B - Condens. Matter Mater. Phys.* **2006**, *74* (15), 2–5.

(35) Saloman, E. B.; Hubbell, J. H.; Scofield, J. H. X-Ray Attenuation Cross Sections for Energies 100 eV to 100 keV and Elements Z = 1 to Z = 92 *At. Data Nucl. Data Tables* **1988**, *38*, 1–196.

(36) Dinelli, F.; Assender, H. E.; Takeda, N.; Briggs, G. A. D.; Kolosov, O. V. Elastic Mapping of Heterogeneous Nanostructures with Ultrasonic Force Microscopy (UFM). *Surf. Interface Anal.* **1999**, *27*, 562–567.

(37) Bosse, J. L.; Tovee, P. D.; Huey, B. D.; Kolosov, O. V. Physical Mechanisms of Megahertz Vibrations and Nonlinear Detection in Ultrasonic Force and Related Microscopies. J. Appl. Phys. Lett **2014**, 115, 144304-1 - 144304-7.

(38) Dinelli, F.; Biswas, S. K.; Briggs, G. A. D.; Kolosov, O. V. Ultrasound Induced Lubricity in Microscopic Contact. *Appl. Phys. Lett.* **1997**, *71,* 1177-1179.

(39) Jaehnike, F.; Pham, D.; Anselmann, R.; Bock, C.; Kunze, U. High-Quality Solution-Processed Silicon Oxide Gate Dielectric Applied on Indium Oxide Based Thin-Film Transistors. *ACS Appl. Mater. Interfaces,* **2015**, 7 (25), pp 14011–14017.

(40) Lenzlinger, M.; Snow, E. H. Fowler - Nordheim Tunneling into Thermally Grown SiO_2. J. Appl. Phys. **1969**, *40*, 278-283.

(41) Jeong, Y.; Pearson, C.; Kim, H.; Park, M.; Kim, H.; Do, L.; Petty, M. C. Optimization of a Solution-Processed SiO_2 Gate Insulator by Plasma Treatment for Zinc Oxide Thin Film Transistors. *ACS Appl. Mater. Interfaces*, **2016**, *8*, 2061–2070.

(42) Robertson, J.; Wallace, R. M. High-K Materials and Metal Gates for CMOS Applications. *Mater. Sci. Eng., R.* **2015**, *88*, 1–41.

(43) Robertson, J. High Dielectric Constant Gate Oxides for Metal Oxide Si Transistors. *Rep. Prog. Phys.* **2005**, *69*, 327–396.

TOC Figure: